

## Molecular Dynamics Simulations on $\beta$ Amyloid Peptide (25-35) in Aqueous Trifluoroethanol Solution

Sangwon Lee and Yangmee Kim\*

*Department of Chemistry and Department of Advanced Fusion Technology, Konkuk University, Seoul 143-701, Korea*

*Received March 3, 2004*

Amyloid peptide ( $A\beta$ ) is the major component of senile plaques found in the brain of patient of Alzheimer's disease.  $\beta$ -amyloid peptide (25-35) ( $A\beta_{25-35}$ ) is biologically active fragment of  $A\beta$ . The three-dimensional structure of  $A\beta_{25-35}$  in aqueous solution with 50% (vol/vol) TFE determined by NMR spectroscopy previously adopts an  $\alpha$ -helical conformation from Ala<sup>30</sup> to Met<sup>35</sup>. It has been proposed that  $A\beta_{25-35}$  exhibits pH- and concentration-dependent  $\alpha$ -helix  $\leftrightarrow$   $\beta$ -sheet transition. This conformational transition with concomitant peptide aggregation is a possible mechanism of plaque formation. Here, in order to gain more insight into the mechanism of  $\alpha$ -helix formation of  $A\beta_{25-35}$  peptide by TFE, which particularly stabilizes  $\alpha$ -helical conformation, we studied the secondary-structural elements of  $A\beta_{25-35}$  peptide by molecular dynamics simulations. Secondary structural elements determined from NMR spectroscopy in aqueous TFE solution are preserved during the MD simulation. TFE/water mixed solvent has reduced capacity for forming hydrogen bond to the peptide compared to pure water solvent. TFE allows  $A\beta_{25-35}$  to form bifurcated hydrogen bonds to TFE as well as to residues in peptide itself. MD simulation in this study supports the notion that TFE can act as an  $\alpha$ -helical structure forming solvent.

**Key Words :**  $A\beta_{25-35}$ , Conformation, Hydrogen bond, TFE, MD simulation

### Introduction

The aggregation of  $\alpha$ -helix-rich proteins into beta-sheet-rich amyloid fibrils is associated with fatal diseases, such as Alzheimer's disease and prion disease. The mechanism of this disease associates with progressive deposition of these amyloid fibrils to form senile plaques.<sup>1,2</sup> During an aggregation process, protein secondary structural elements,  $\alpha$ -helices undergo conformational changes to  $\beta$ -sheets.<sup>3,4</sup> The main component of plaques found in human patients suffering from Alzheimers disease is a small peptide,  $\beta$ -amyloid A4 ( $A\beta$ ), of 39-43 amino acids derived from amyloid A4 precursor protein (APP) by proteolytic cleavage.<sup>1,6</sup> There are growing interests in neurotoxicity of this hydrophobic peptide  $A\beta$  and progressive cerebral deposition of  $A\beta$  appears to be at least the necessary event in the pathogenesis of the disease.<sup>7</sup>  $A\beta$  includes 28 residues corresponding to an extra cellular domain, and the rest of the protein constitutes a transmembrane region.<sup>8</sup>  $A\beta_{25-35}$  having an amino acid sequence of Gly-Ser-Asn-Lys-Gly-Ala-Ile-Ile-Gly-Leu-Met that contains both hydrophilic domain (Ser<sup>26</sup>-Gly<sup>29</sup>) and six hydrophobic residues of transmembrane region has been reported to have biologically active fragment and contribute to aggregation.<sup>9-12</sup> Also it was reported that the biological activity of  $A\beta_{25-35}$  is not reduced as compared to full-length of  $A\beta$ .<sup>9-12</sup>

Various high-resolution structural studies have been executed using nuclear magnetic resonance (NMR) spectroscopy upon full length, N-terminal or C-terminal fragments

of  $A\beta$  under a variety of conditions.<sup>13-19</sup> Circular dichroism (CD) spectroscopy and infrared (IR) spectroscopy studies of this peptide and its fragment suggest that the secondary structure content of these peptides is strongly dependent on solution conditions.<sup>20-27</sup> It has been proposed by CD spectroscopy that  $A\beta$  exhibits pH- and concentration-dependent  $\alpha$ -helix  $\leftrightarrow$   $\beta$ -sheet transition<sup>24</sup> and 25-35 fragments shows lipid-induced reversible random-coil  $\leftrightarrow$   $\beta$ -sheet transition.<sup>20,21</sup> This conformational transition with concomitant peptide aggregation is a possible mechanism of plaque formation.

According to our previous CD studies,  $A\beta_{25-35}$  in SDS micelle has a single minimum at 215 nm, which is the characteristic of the  $\beta$ -sheet structure while  $A\beta_{25-35}$  has a random coil conformation in aqueous buffer.<sup>13</sup> Surprisingly, it adopts  $\alpha$ -helical conformation without aggregation in the presence of trifluoroethanol (TFE). TFE is known as a secondary-structure-inducing agent. Since influence of TFE on the conformation of peptides is not well understood, characterization of the effects of TFE is important to understand protein folding. Here, in order to gain more insight into the mechanism of  $\alpha$ -helix formation of  $A\beta_{25-35}$  peptide in TFE, which particularly stabilizes  $\alpha$ -helical conformation, we studied the secondary-structural elements of the  $A\beta_{25-35}$  peptide in TFE aqueous solution by molecular dynamics simulations.

### Experimental Section

All of the calculations were performed using CHARMM program.<sup>28-31</sup> The molecular dynamics simulation was performed using explicit solvent molecules at a temperature of 300 K for the time length of 1.5 ns. The starting

\*To whom correspondence should be addressed. Phone: +82-2-450-3421, Fax: +82-2-447-5987, e-mail: ymkim@konkuk.ac.kr

conformation of A $\beta$ 25-35 was taken from the restrained-minimized average structure determined in our previous work by NMR experiments that were conducted in 50% aqueous TFE solution.<sup>13</sup> In order to solvate this structure completely, a cubic box consisting of 500 water molecules and 137 TFE molecules, with a length of 31 Å in each dimension was created. This box was equilibrated by 100ps molecular dynamics after randomly placing of solvent molecules. The parameters for the polypeptide chain in peptide and TIP3P water model for simulating water molecules were used from the standard parameter set version 19 supplied with CHARMM.<sup>32,33</sup> Additional parameters for TFE molecules were taken from the previous work.<sup>31-36</sup> The 'extended atom' representation was used for TFE molecules, so that only hydrogen atoms having possibility of involving hydrogen bonds were included in the calculations. Periodic boundary conditions were applied after solvation of the peptide. Dielectric constant was set to unity and the nonbonded distance cutoff was set to 12 Å. The nonbonded interactions were smoothed between 8 and 11 Å using switch function. The starting conformation of A $\beta$ 25-35 was solvated in the TFE/H<sub>2</sub>O cubic box and a number of solvent molecules with any atom closer than 2.6 Å to any of the peptide atoms were removed, leaving a total of 446 water molecules and 110 TFE molecules in the system. Then, 500 steps of steepest decent minimization were carried out with the peptide harmonically constrained to its original coordinates to eliminate any unfavorable close contacts and geometric strain in the system. During the first 40ps of MD simulation, the peptide was harmonically constrained to its original position, allowing the solvent molecules to equilibrate further. The complete system was gradually heated to 300 K during the first 30ps and equilibrated for 10ps. The constraints on the peptide were removed after the first 40ps and the system was equilibrated for 30ps. The intermediate structures generated during MD simulation were saved every 0.5ps. All covalent bonds containing the hydrogen atoms were constrained using SHAKE algorithm<sup>37</sup> with the tolerance of  $10^{-10}$  Å. Verlet algorithm<sup>38</sup> was used for the MD simulation using a time step of 1fs. The total length of the simulation was 1.5 ns.

## Results and Discussion

### RMSD as a function of time in MD simulations.

According to our previous CD study, A $\beta$ 25-35 has a random coil conformation in aqueous buffer, while it adopts  $\alpha$ -helical conformation without aggregation in the presence of TFE.<sup>13</sup> Figure 1 shows the superposition of 20 low energy structures on the backbone atoms from Ala<sup>30</sup> to Leu<sup>34</sup> of A $\beta$ 25-35 in TFE/water (1 : 1, vol/vol) solution determined by NMR spectroscopy and they converged well. Lowest energy structure was utilized for the starting structure of MD simulation.<sup>13</sup>

Figure 2 shows the RMS deviations from the starting structure during 1.5 ns MD simulations. The RMSD values of the protein backbone atoms between the structures

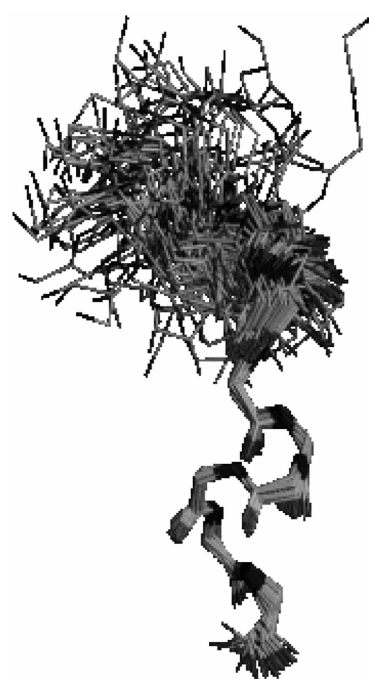


**Figure 1.** Final 20 low energy structures of A $\beta$ 25-35 in TFE/water solution superimposed on Ala<sup>30</sup>-Leu<sup>34</sup>.<sup>13</sup>

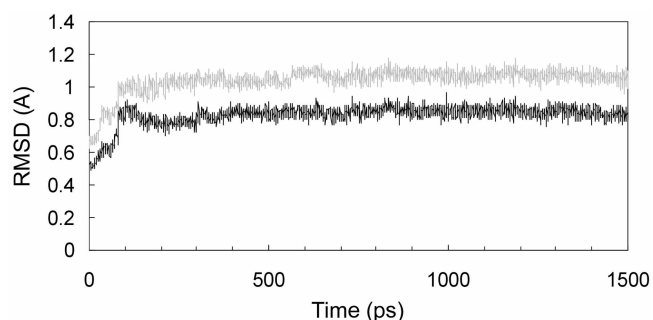


**Figure 2.** Rms deviations of A $\beta$ 25-35 from the starting structure during 1.5ns MD simulation in TFE/H<sub>2</sub>O (1 : 1, v/v). The peptide conformation was stored every 50fs during MD simulation. Black line is the value for the backbone atoms and gray line is the value for the all heavy atoms of the peptide.

resulting from the simulations and the starting structure are compared in Figure 2. In the simulations a rapid initial increase of the RMSD was observed during the first 100 ps. RMSD values in a TFE/water mixed solvent tended to be relatively constant after 100ps including heating and equilibrium periods. All structures were fit well against the equilibrated structure obtained after the heating stage in order to remove effects from translational and rotational shifts. The RMSD values of the all heavy atoms including the side chain atoms are shown in gray lines and are slightly higher than those of backbone atoms. This implies that the side chains in A $\beta$ 25-35 show bigger structural flexibilities than the backbone atoms during the MD simulation.

**Comparison of results of NMR experiment and MD simulation.** Table 1 shows the comparison of the distance between peptide amide protons and Ca protons from NMR

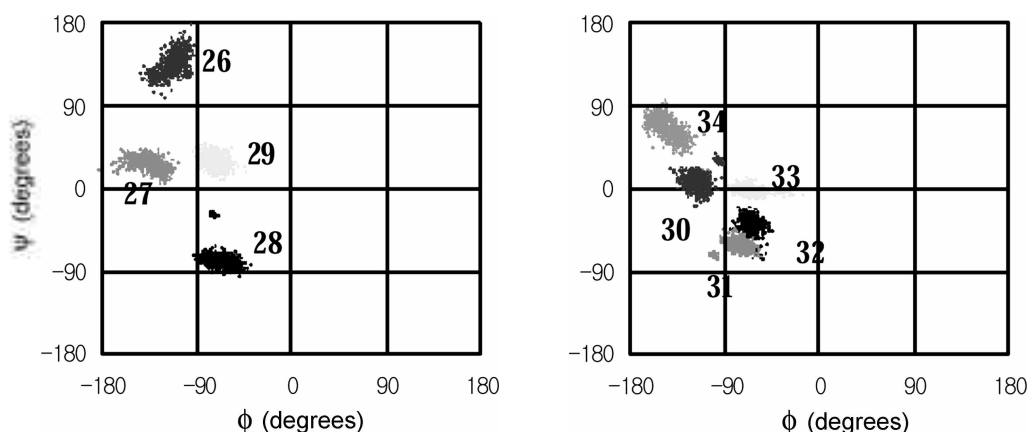
**Table 1.** Comparison of distances between peptide amide protons and C $\alpha$  protons from NMR experiments and from MD simulation

Distances		NMR experiments <sup>a</sup>	MD simulation ( $\text{\AA}$ ) <sup>b</sup>
NH	C $\alpha$ H		
28	26	M	3.75 + 0.17
29	27	M	3.82 + 0.25
30	28	W	4.22 + 0.14
34	31	M	3.13 + 0.20
35	32	M	4.41 + 0.31
34	30	W	3.65 + 0.21

<sup>a</sup>From Ref (13). S, M, and W represent experimentally observed NOESY peaks having intensities of strong (1.8–2.7  $\text{\AA}$ ), medium (1.8–3.5  $\text{\AA}$ ), and weak 1.8–5.0  $\text{\AA}$ , respectively. <sup>b</sup>Distances were presented as average values  $\pm$  standard deviations from average values.

experiments and MD simulations. Starting structure of A $\beta$ 25–35 has an  $\alpha$ -helical structure from Ala30 to Met35. NOE intensities can be divided into three classes (strong, medium, and weak) with distance ranges of 1.8–2.7, 1.8–3.5, and 1.8–5.0  $\text{\AA}$ , respectively.  $\alpha$ -helical conformations are retained during the MD simulations but the Met<sup>35</sup> at the C-terminus fluctuates a lot.  $d\alpha\text{N}(i,i+3)$  connectivity for Ile<sup>31</sup> C $\alpha$ H–Leu<sup>34</sup> NH and  $d\alpha\text{N}(i,i+4)$  connectivity for Ala<sup>30</sup> C $\alpha$ H–Leu<sup>34</sup> NH, which was the characteristics for  $\alpha$ -helix were retained during the MD simulations as shown in this table. During the simulations the flexibilities of the C-terminal part was increased and distance between Ile<sup>32</sup> and Met<sup>35</sup> becomes longer because of the structural fluctuations at C-terminus.

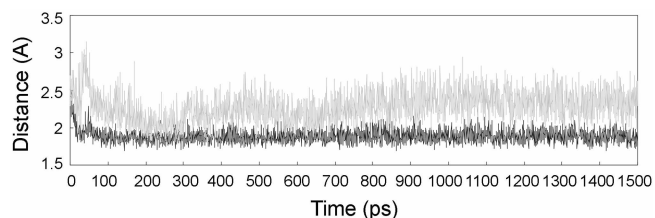
**Dihedral angles  $\Phi$ ,  $\Psi$  plots.** The fluctuations of the backbone dihedral angles are shown in Figure 3. The scattering of the  $\Phi$ ,  $\Psi$  angles in plots can be used as an information about the fluctuations of the secondary structural elements. For each residue, the 200 structures collected during the MD simulations are represented in the figure. Figure 3 shows that all residues fall into either  $\alpha$ -helical region or in generously allowed region and stays well around the initial structure. Since the flexibilities increase at both ends of the peptide a lot, it shows only values for the residues from 26 to 34. Residues which satisfy helical conformations in the initial structures in TFE/water solutions are plotted in Figure 3B

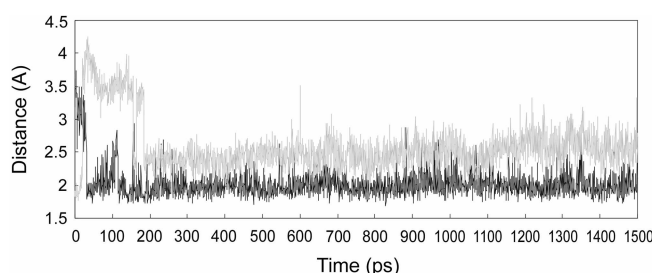
**Figure 3.**  $\Phi$ ,  $\Psi$  plot of A $\beta$ 25–35 during MD simulation in TFE/H<sub>2</sub>O (1 : 1, v/v).

and the rest of the residues are plotted in Figure 3A. In Figure 3B,  $\Phi$ ,  $\Psi$  angles from the residues for Ala<sup>30</sup>, Ile<sup>31</sup>, Ile<sup>32</sup>, and Gly<sup>33</sup> retains  $\alpha$ -helical structures well and located in the most favored regions for  $\alpha$ -helical structure in  $\Phi$ ,  $\Psi$  plot during MD simulations.

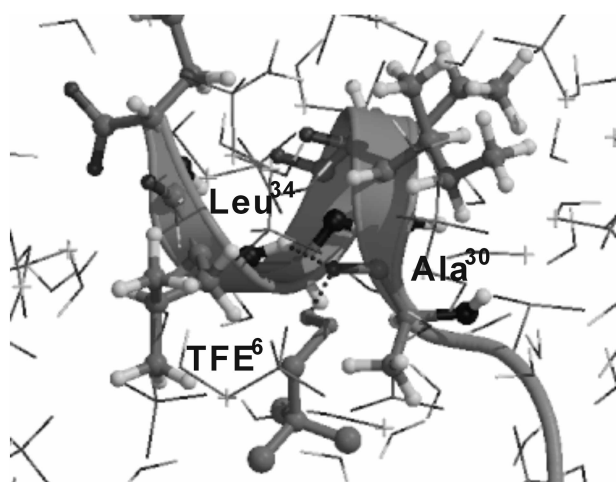
**Hydrogen bonds in A $\beta$ 25–35.** Major factors for protein stabilization are hydrogen bonds, which play an important role in the folding process. For the stability of helix, the backbone hydrogen bond, C=O $\cdots$ H–N ( $i$ – $i$ +4), between amino acid  $i$  and amino acid  $i$ +4 are crucial. The distance between the donor-acceptor should be less than 2.5  $\text{\AA}$ . A stable hydrogen bond is present most of the time between C=O in Ala<sup>30</sup> and N–H in Leu<sup>34</sup> during the simulation and retains the distance less than 2.5  $\text{\AA}$  which can prove the existence of stable one turn  $\alpha$ -helix between Ala<sup>30</sup> and Leu<sup>34</sup>. From Lys<sup>28</sup> to Ala<sup>30</sup>, which is not in the helical region,  $i$ – $i$ +2 connectivity observed in NMR experiments was maintained during the MD simulations as shown in Figure 4.

Figure 5 shows that distance time course for the intermolecular distances between A $\beta$ 25–35 and TFE molecules during MD simulation in TFE/H<sub>2</sub>O. During first 50 ps, there is no hydrogen bond between peptide and TFE molecules. After 50 ps, a hydrogen bond between C=O of A $\beta$ 25–35 and O–H of TFE are formed. Hydrogen bond between C=O of Ala<sup>30</sup> and O–H of TFE<sup>6</sup> is depicted by black solid line and that for Ile<sup>32</sup>–TFE<sup>7</sup> is depicted by gray solid lines. C=O of Ala<sup>30</sup> and N–H of Ile<sup>34</sup> has a hydrogen bond as shown in

**Figure 4.** Distance time course for the intrapeptide distances of A $\beta$ 25–35 during MD simulation in TFE/H<sub>2</sub>O. Black line and gray line represent the distance between C=O of Lys<sup>29</sup> and N–H of Ala<sup>30</sup> and the distance between C=O of Ala<sup>30</sup> and N–H of Leu<sup>34</sup>, respectively.



**Figure 5.** Distance time course for the intermolecular distances between A $\beta$ 25-35 and TFE molecules during MD simulation in TFE/H<sub>2</sub>O. Distances between C=O of A $\beta$ 25-35 and O-H of TFE molecules are depicted with black solid line: Ala<sup>30</sup>-TFE<sup>6</sup> and with gray solid line: Ile<sup>12</sup>-TFE<sup>7</sup>.



**Figure 6.** Final snapshot at 1.5ns after MD simulation. The hydrogen bonds between C=O of Ala<sup>30</sup> and N-H of Leu<sup>34</sup> and the hydrogen bond between C=O of Ala<sup>30</sup> and O-H of TFE<sup>6</sup> are depicted with dotted lines.

Figure 4 and at the same time C=O of Ala<sup>30</sup> has a hydrogen bond with O-H of TFE<sup>6</sup> as shown in Figure 5. In mixed solvents of water and TFE, the properties will be intermediate between those of the two pure solvents. Therefore, the TFE concentration increases, charge interactions in peptide might be expected to become more important due to a lowering of the dielectric constant. The relative stabilities of the hydrogen bonds, C=O...H-N (i-i-4) in the  $\alpha$ -helix might also be changed by the solvent composition. A breaking of hydrogen bonds of the peptide backbone, which is characterized by the insertion of the water molecules, was not observed during the simulations. As shown in Figure 6, there are hydrogen bonds between OH group of TFE and peptide backbone as well as those between the peptide backbone atoms. C=O of Ala<sup>30</sup> form bifurcated hydrogen bonds with O-H of TFE<sup>6</sup> as well as with N-H of Leu<sup>34</sup>.

### Conclusion

CD measurement in our previous study indicates that A $\beta$ 25-35 in SDS micelle adopts  $\beta$ -sheet conformation at pH 4.<sup>15</sup> Previous CD studies in phospholipid vesicles<sup>21</sup> also

describe that A $\beta$ 25-35 exhibits a reversible random coil  $\leftrightarrow$   $\beta$ -sheet structure induced by negatively charged vesicles. In contrast, in TFE/water solution, A $\beta$ 25-35 forms a stable  $\alpha$ -helical conformation from 30 to 35.<sup>15</sup> Water molecule destabilizes the  $\alpha$ -helix in the peptide due to the strong interactions between the charged atoms in peptide and water. Dielectric constant of TFE is about one-third that of water, resulting in a strengthening of interactions between charged groups in the peptides. TFE is much weaker base than water resulting in a weaker capacity for accepting protons in hydrogen bonds. TFE has only one O-H group and has a much larger size than water. TFE/water mixed solvent has reduced capacity for forming hydrogen bond to the peptide compared to pure water solvent. Therefore, TFE forms hydrogen bonds to A $\beta$ 25-35 and allows A $\beta$ 25-35 to maintain the intramolecular hydrogen bond. In conclusion,  $\alpha$ -helical secondary structure elements in A $\beta$ 25-35 determined from NMR spectroscopy in TFE/water mixed solvent are preserved during the MD simulation. TFE allows the peptide to form bifurcated hydrogen bonds to TFE as well as to peptide itself. MD simulation in this study supports the notion that TFE acts an  $\alpha$ -helical structure forming solvent. Since it is important to develop a tool to control the amyloid deposition observed in Alzheimers disease patients, it will be meaningful to study how to manipulate the condition to promote the  $\alpha$ -helical conformation of A $\beta$ 25-35.

**Acknowledgement.** This work was supported by Konkuk University in 2003.

### References

- Chromy, B. A.; Nowak, R. J.; Lambert, M. P.; Viola, K. L.; Chang, L.; Velasco, P. T.; Jones, B. W.; Fernandez, S. J.; Laco'r, P. N.; Horowitz, P.; Finch, C. E.; Krafft, G. A.; Klein, W. L. *Biochemistry* **2003**, *42*, 12749.
- Hardy, J. A.; Higgins, J. A. *Science* **1992**, *256*, 184.
- Hardy, J. A. *Proc. Natl. Acad. Sci. USA* **1997**, *94*, 2095.
- Chiti, F.; Stefani, M.; Taddei, N.; Ramponi, G.; Dobson, C. M. *Nature* **2003**, *424*, 805.
- Hirschfeld, G. M.; Hawkins, P. N. *Int. J. Biochem. Cell Biol.* **2003**, *35*, 1608.
- Kang, J.; Lemaire, H. G.; Unterbeck, A.; Salbaum, M. N.; Masters, C. L.; Grzeschik, K. H.; Multhaup, G.; Beyreuther, K.; Mueller-Hill, B. *Nature* **1987**, *325*, 733.
- Selkoe, D. J. *Trends. Neurosci.* **1993**, *16*, 403.
- Fraser, P. E.; Nguyen, J. T.; Surewicz, W. K.; Kirschner, D. A. *Biophys. J.* **1991**, *60*, 1190.
- Mattson, M. P.; Cheng, B.; Davis, D.; Bryant, K.; Lieberburg, I.; Rydel, R. E. *J. Neurosci.* **1992**, *12*, 376.
- Pike, C. J.; Burdick, D.; Walencewicz, A. J.; Glabe, C. G.; Cotman, C. W. *J. Neurosci.* **1993**, *13*, 1676.
- Pike, C. J.; Walencewicz, A. J.; Kosmoski, J.; Cribbs, D. H.; Glabe, C. G.; Cotman, C. W. *J. Neurochem.* **1995**, *64*, 253.
- Yankner, B. A.; Duffy, L. K.; Kirschner, D. A. *Science* **1990**, *250*, 279.
- Lee, S.; Suh, Y.-H.; Kim, S.; Kim, Y. *J. Biomol. Struct. Dyn.* **1999**, *17*, 381.
- Srinivasan, R.; Jones, E. M.; Liu, K.; Ghiso, J.; Marchant, R. E.; Zagorski, M. G. *J. Mol. Biol.* **2003**, *333*(5), 1003.
- Bond, J. P.; Deverin, S. P.; Inouye, H.; El-Agnaf, O. M.; Tector, M. M.; Kirschner, D. A. *J. Struct. Biol.* **2003**, *141*, 156.

16. Talafoos, J.; Marcinowski, K. J.; Klopman, G.; Zagorski, M. G. *Biochemistry* **1994**, *33*, 7788.
  17. Sorimachi, K.; Craik, D. J. *Eur. J. Biochem.* **1994**, *219*, 237.
  18. Lee, J. P.; Stimson, E. R.; Ghilardi, J. R.; Mantyh, P. W.; Lu, Y.; Felix, A. M.; Llanos, W.; Behbin, A.; Cummings, M.; Crieckinge, M. V.; Timms, W.; Maggio, J. E. *Biochemistry* **1995**, *34*, 5191.
  19. Kohno, T.; Kobayashi, K.; Maeda, T.; Sato, K.; Takashima, A. *Biochemistry* **1996**, *35*, 16094.
  20. Terzi, E.; Holzemann, G.; Seelig, J. *Biochemistry* **1994**, *33*, 1345.
  21. Terzi, E.; Holzemann, G.; Seelig, J. *Biochemistry* **1994**, *33*, 7434.
  22. Lin, S. Y.; Chu, H. L. *Int. J. Biol. Macromol.* **2003**, *32*, 173.
  23. Ding, F.; Borreguero, J. M.; Buldyrey, S. V.; Stanley, H. E.; Dokholyan, N. V. *Proteins* **2003**, *53*(2), 220.
  24. Otvos, Jr., L.; Szendrei, G. J.; Lee, J. M.; Mantsch, H. H. *Eur. J. Biochem.* **1993**, *211*, 249.
  25. Hollosi, M.; Otvos, Jr., L.; Kajtar, J.; Perczel, A.; Lee, V. M. *Peptide Res.* **1989**, *2*, 109.
  26. Halverson, K.; Fraser, P. E.; Kirschner, D. A.; Lansbury, Jr., P. T. *Biochemistry* **1990**, *29*, 2639.
  27. Soto, C.; Castaño, E. M.; Frangione, B. F.; Inestrosa, N. C. *J. Biol. Chem.* **1995**, *270*, 3063.
  28. Molecular Simulation Inc.: San Diego, CA.
  29. Cheong, Y.; Shim, G.; Kang, D.; Kim, Y. *J. Mol. Struct.* **1999**, *475*, 219.
  30. Shim, G.; Lee, S.; Kim, Y. *Bull. of Korean Chem. Soc.* **1997**, *18*, 415.
  31. Shim, G.; Shin, J.; Kim, Y. *Bull. of Korean Chem. Soc.* **2004**, *25*, 198.
  32. Jorgensen, W. L.; Chandrasekhar, J.; Madura, J. D.; Impey, R. D.; Klein, M. L. *J. Chem. Phys.* **1989**, *79*, 926.
  33. Jois, S. D.; Hughes, R.; Siahaan, T. J. *Biomol. Struct. Dyn.* **1999**, *17*(3), 429.
  34. Van Buuren, A. R.; Berendsen, H. J. C. *Biopolymers* **1993**, *33*, 1159.
  35. Loof, H. D.; Nilsson, L.; Rigler, R. *J. Am. Chem. Soc.* **1992**, *114*, 4028.
  36. Sticht, H.; Willbold, D.; Rosch, P. *J. Biomol. Struct. Dyn.* **1994**, *12*(1), 19.
  37. Van Gunsteren, W. F.; Berendsen, H. J. C. *Mol. Phys.* **1977**, *34*, 1311.
  38. Verlet, L. *Phys. Rev.* **1967**, *159*, 98.
-